Electronic Supplementary Material (ESI) for Polymer Chemistry.

Supporting information

3D printed objects obtained by combination of radical photopolymerization and photo sol-gel reaction: towards reinforced thermomechanical properties

Lucile Halbardier, Céline Croutxé-Barghorn*, Emile Goldbach, Anne-Sophie Schuller, Xavier Allonas

I. Experimental section

Nuclear magnetic resonance in liquid state – ^{1}H-NMR

The sample was prepared by mixing 0.2 ml of MAPTMS in 2ml of $CDCl_3$. The ^{1}H-NMR spectra was recorded at room temperature with a Bruker Advance 400 spectrometer equipped with 5-mm Z-gradient quadruple nucleus probe for routine spectroscopy. A recycling delay of 10s was selected and the spectra was acquired with 16 scans. The spectra of the MAPTMS was normalized with the residual proton signal of the solvent $CHCl_3$ at 7.26 ppm.

Differential Scanning Calorimetry - DSC

The glass transition temperature of the printed material S_{100} was evaluated using a DSC (DSC 25, TA Instruments). 10 to 15 mg of the cut sample were introduced in hermetically sealed pans. The heat flow was recorded between -90 and 210°C with a heating rate of 10°C/minute. Tangents of the curve were plotting to evaluate the Tg.

Determination of Jacobs parameters for the photosensitive resins

The depth penetration of the light (Dp) has to be superior to the layer thickness and inferior to 4 layers to limit the light diffusion and guaranty a good resolution. According to the Jacobs equation[1–3], the critical energy, Ec, required to cure the resin to its gel point and the depth penetration Dp of the light were determined at 0.9 mJ/cm² and 95 µm for S_{100} and 3.7 mJ/cm² and 126 µm for $S_{80}M_{20}$.

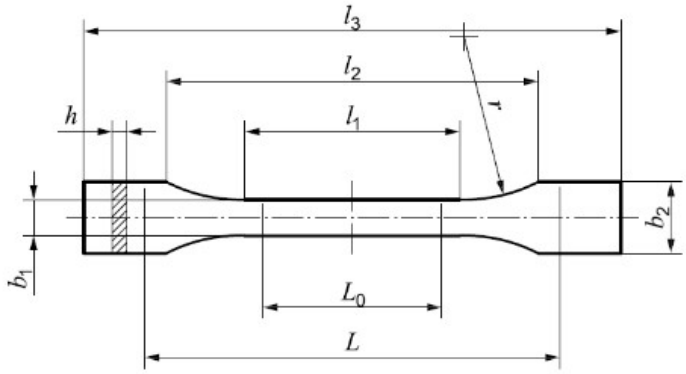

3D printing of the sample

Fig. S1. Dimensions of the 1BA sample from the standard ISO 527-2.

Table S1. Dimensions of the 1BA sample from the standard ISO 527-2.

Sample	1BA
l_3 Total length	≥ 75mm , adjusted at 116mm
l_1 Length of the narrow part with parallel faces	30mm
r Radius	≥ 30mm
l_2 Distance between wide parts with parallel faces	58mm
b_1 Width at ends	10mm
b_2 Width of narrow part	5mm
h Thickness	≥ 2mm, adjusted at 4mm
L_0 Reference length	25mm
L Initial distance between the jaws	l_2

Attenuated Total Reflection - Fourier Transform Infrared Spectroscopy

Different $Conv_{C=C}$ values were observed on the surface of the sample between the plate side where the first layer was printed and the vat side, corresponding to the last printed layer. This can be explained by a difference of light dose received by each layer. The $Conv_{C=C}$ on the surface was determined by an average of 3 values obtained on each face and on 2 samples for each formulation. The 1BA samples were cuted to assess the $Conv_{C=C}$ on the inner part of the printed material with an average of two measurements for two samples.

II. Additional measurements

ATR-FTIR spectra of uncured and printed materials S_{100}

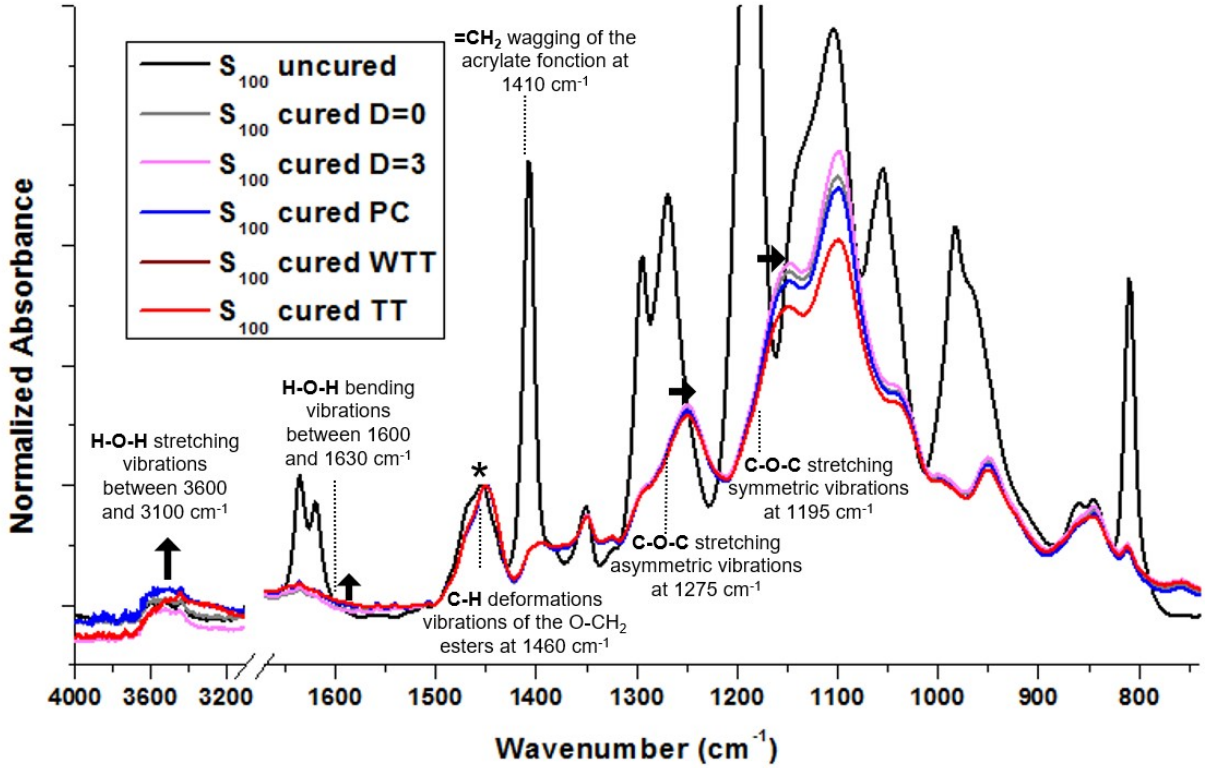

Fig. S2. ATR-FTIR spectra of the uncured formulation and of the center of 4mm S_{100} printed samples. Measurements were made directly after the 3D printing (D=0), 3 days after (D=3) or after post-treatments (PC, WTT or TT). *Spectra were normalized to the reference band at 1460 cm^{-1}.

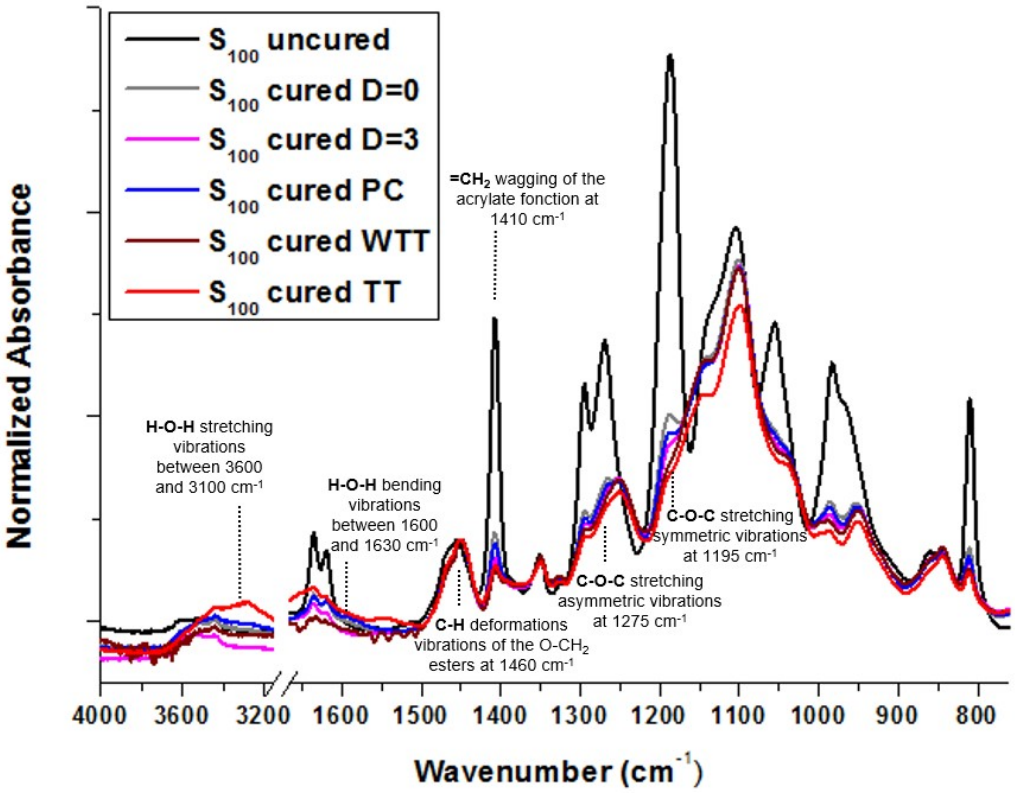

Fig. S3. ATR-FTIR spectra of the uncured formulation and of the last printed layer of the S_{100} printed samples. Measurements were made directly after the 3D printing (D=0), 3 days after (D=3) or after post-treatments (PC, WTT or TT). Spectra were normalized to the reference band at 1460 cm^{-1}.

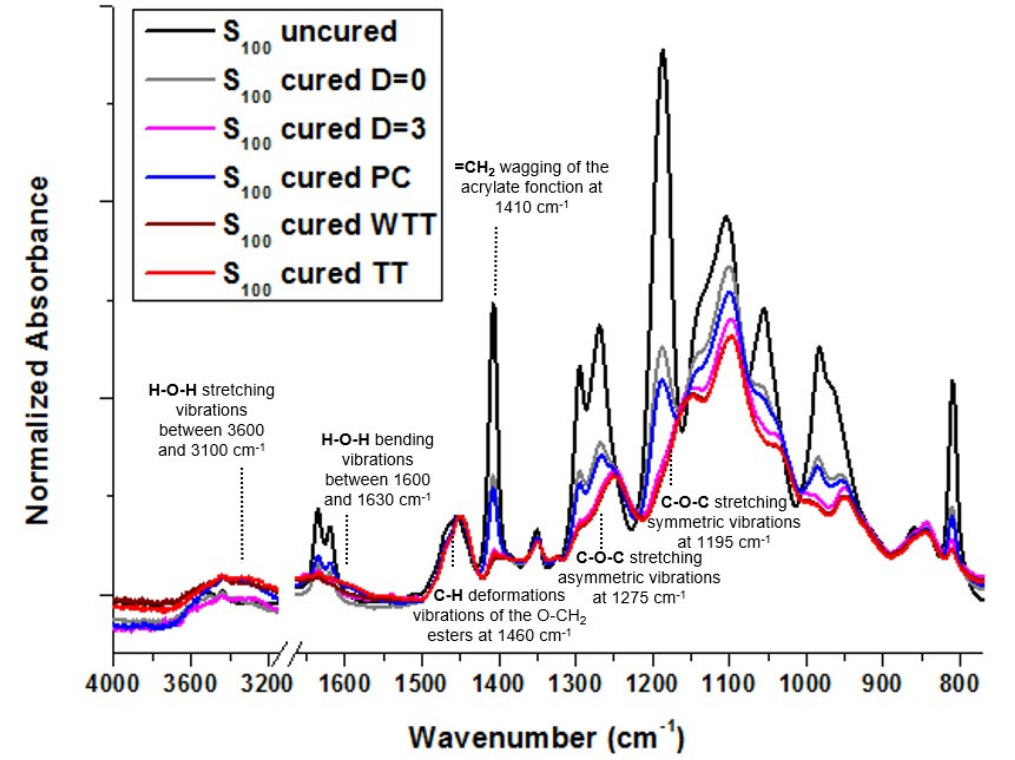

Fig. S4. ATR-FTIR spectra of the uncured formulation and of the first printed layer of the S_{100} printed samples. Measurements were made directly after the 3D printing (D=0), 3 days after (D=3) or after post-treatments (PC, WTT or TT). Spectra were normalized to the reference band at 1460 cm^{-1}.

Table S2. Area of the ATR-FTIR band between 3100-3600 cm^{-1} for the printed S_{100} sample on the outer surfaces (first and last printed layer) without PT (D=0 and D=3) and with PT (PC, WTT, TT).

3D printed S_{100} sample	Area of the band 3100 and 3600 cm^{-1}	
	First printed layer	Last printed layer
Without PT, D=0	2.09 ± 0.23	1.17 ± 0.61
Without PT, D=3	2.30 ± 0.29	1.04 ± 0.11
PC	4.01 ± 0.54	1.74 ± 0.45
WTT	1.39 ± 0.80	0.43 ± 0.23
TT	2.48 ± 0.43	3.00 ± 0.14

DMA investigation of the shoulder at -80°C

Photosensitive resins composed by PEG400DA or TCDDMDA were cured with 1 wt% TPO at 385 nm and 70 mW/cm². The respective 170 µm thick polymer films were analyzed by DMA. The tan δ curves were compared to those obtained for S_{100} after 3D printing (D=0) and after WTT+PC (Figure S3).

A shoulder appears at -80°C for the cured PEG400DA and S_{100} samples. Since its presence is also observed after WTT + PC, which leads to complete acrylate conversion (Table 4), it does not correspond to uncured PEG400DA. This peak may be possibly attributed to β relaxation, which appears at lower temperatures than the α relaxation. The relaxation temperature Tα and the height of the tan δ curves H are reported Table S2.

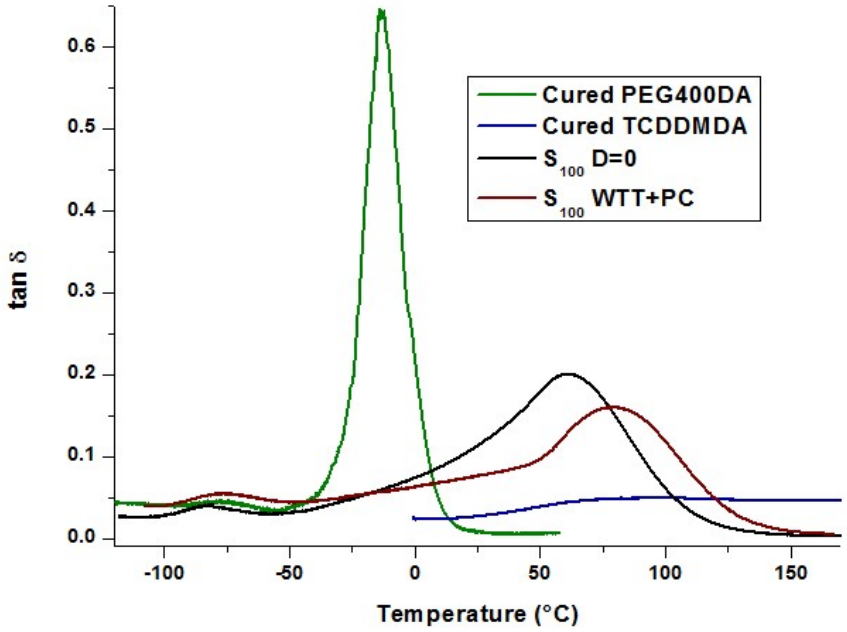

Fig. S5. Tan δ of the cured monomer PEG400DA, TCDDMDA and S_{100} directly after the 3D printing (D=0) and after WTT + PC post-treatment.

Table S3. Tα and H for the cured monomers TCDDMDA and PEG400DA and the printed materials S_{100} and $S_{80}M_{20}$.

	Tα (°C)	H
Cured TCDDMDA	97	0.05
Cured PEG400DA	-13	0.60
Printed material S_{100}	62	0.20
Printed material $S_{100\ WTT+PC}$	41	0.21

Integration of the area band characteristic of the methanol, water and silanol and condensed functions

The areas of the ATR-FTIR bands were normalized to a reference band at 1460 cm^{-1} (attributed to C-H deformation vibration of the -O-CH_2 groups).

Table S4. Areas obtained after integration of the ATR-FTIR band at 3100-3600 cm^{-1} and the shoulder at 1030 cm^{-1} for the uncured $S_{80}M_{20}$ and the inner part of the printed material without PT (D=0, D=3, D=7).

	Area of the band	
	O-H stretching 3600 and 3100 cm^{-1}	**Si-O-Si deformation Shoulder at 1030 cm^{-1}**
Uncured $S_{80}M_{20}$	0	0
Without PT, D=0	1.52 ± 0.22	0.03 ± 0.01
Without PT, D=3	2.59 ± 0.71	0.08 ± 0.05
Without PT, D=7	5.23 ± 0.71	0.16 ± 0.04

DMA of the printed material $S_{80}M_{20}$ without PAG compared to S_{100}

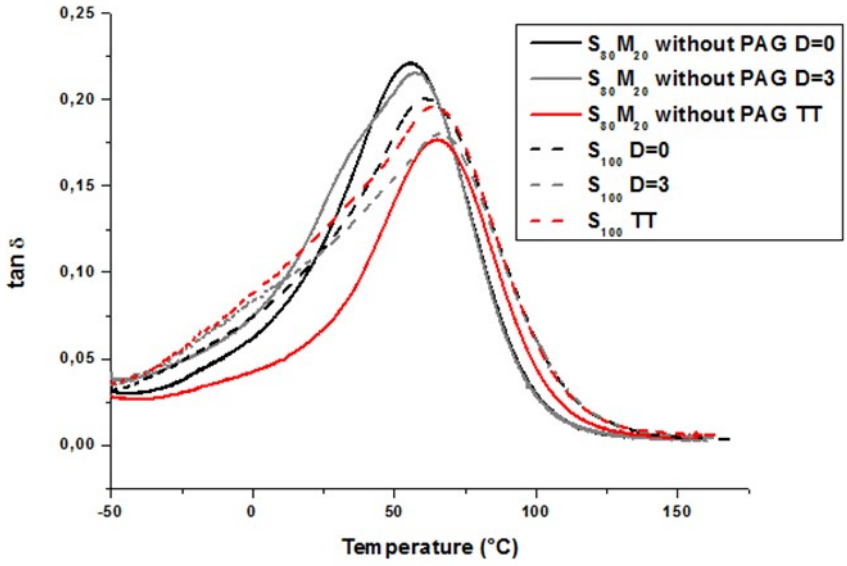

Fig. S6. Evolution of tan δ measured by DMA for the $S_{80}M_{20}$ samples without PAG compared to the S_{100} samples directly after the 3D printing (D=0), 3 days later (D=3) and with a TT.

^{1}H-NMR of the uncured MAPTMS and estimation of the initial condensation degree

The liquid ^{1}H-NMR on the MAPTMS shows two chemical shifts at 3.55 ppm and 3.54 ppm respectively attributed to T^0 and T^1 species[4,5] (**Figure S4**). Their relative ratio was estimated from the integration of the methyl group of the methanol created during the hydrolysis and condensation at 3.46 ppm. T^0 and T^1 amount was assessed at 97.5% and 2.5% respectively. The condensation degree of the liquid MAPTMS was evaluated at 0.8% that was considered as negligible.

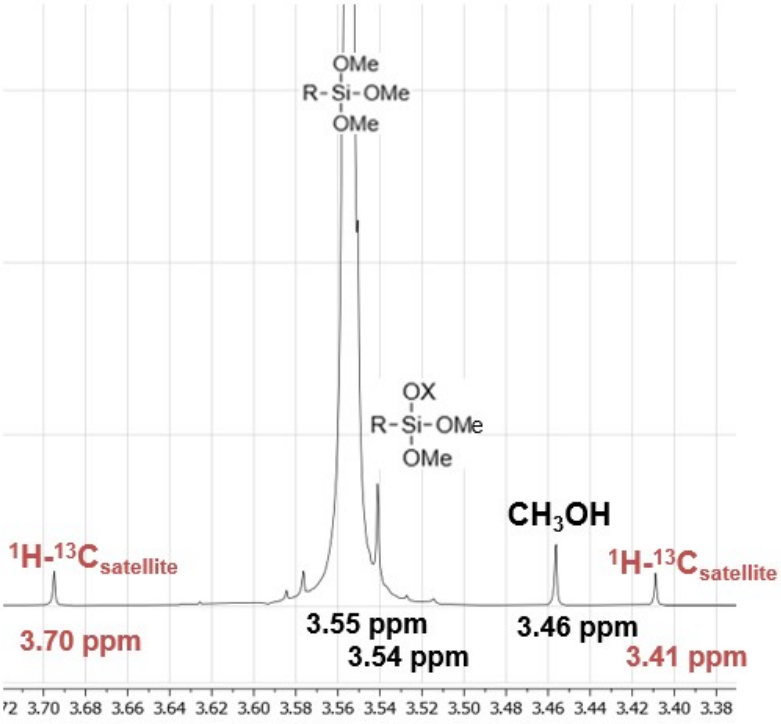

Fig. S7. ^{1}H-NMR Spectra of the liquid MAPTMS between 3.70 and 3.38 ppm.

$$\%_{CH_3-OH} = \%_{molecule\ T^1} = \frac{2}{I_{ref}} * \frac{I_{CH_3-OH}}{3}$$

With I_{CH_3-OH}, the area of the chemical shift at 3.46 ppm and I_{ref}, the area of the reference chemical shift at 4.10 ppm corresponding to the methylene groups –(**CH_2**)-O-C(O)-C(CH_3)=CH_2 into the MAPTMS.

Stabilization of the viscoelastic behaviour of the printed material $S_{80}M_{20}$ followed by DMA

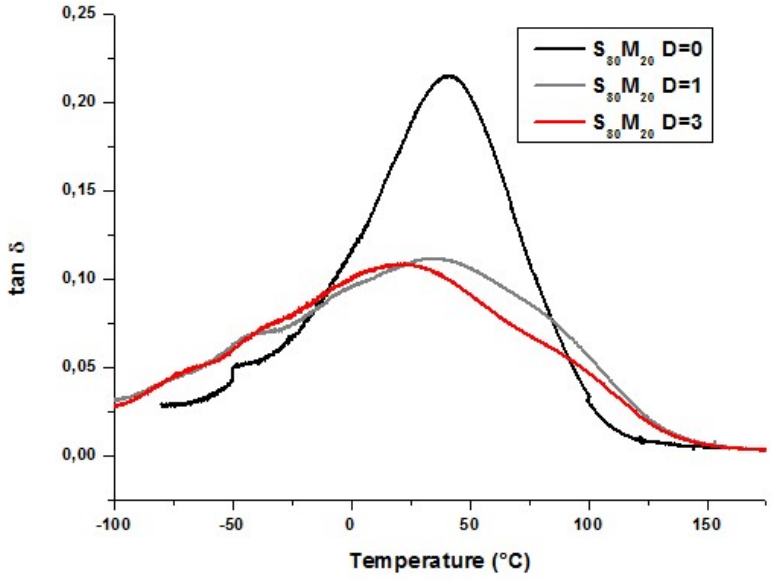

Fig. S8. Evolution of tan δ measured by DMA for $S_{80}M_{20}$ directly after the 3D printing (D=0), 1 day after (D=1) and 3 days later (D=3).

DMA of the printed materials $S_{80}M_{20}$ and S_{100} with or without post-treatment

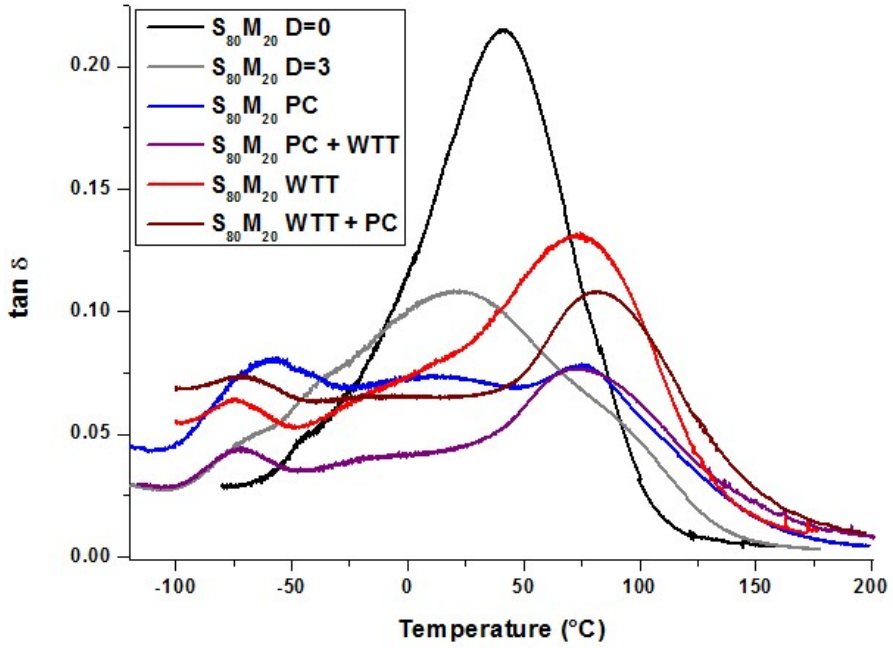

Fig. S9. Tan δ curves of $S_{80}M_{20}$ 3D printed samples directly and 3 days after printing, and after various post-treatments (PC, PC + WTT, WTT, WTT + PC).

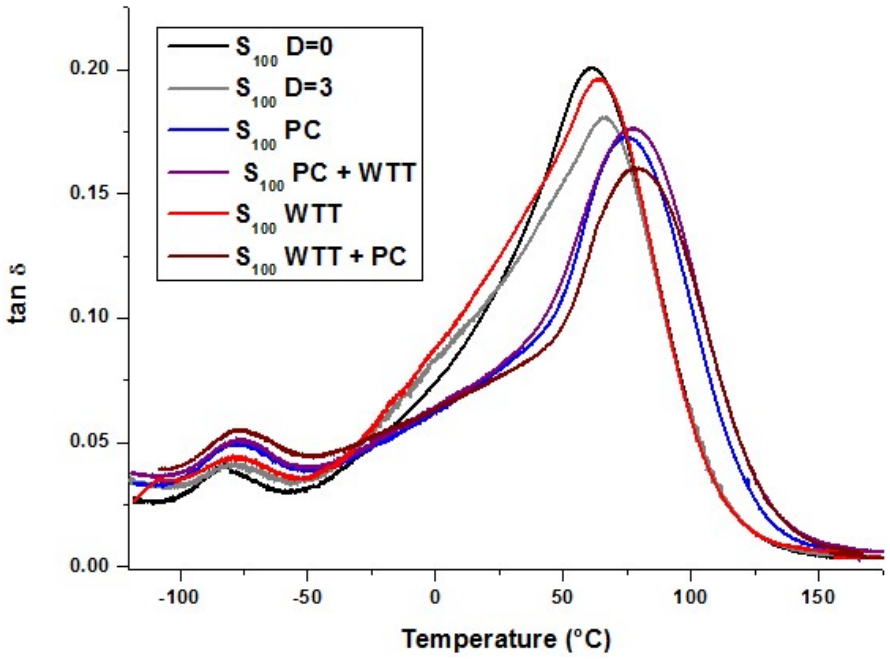

Fig. S10. Tan δ curves of S_{100} 3D printed samples directly and 3 days after printing, and after various post-treatments (PC, PC + WTT, WTT, WTT + PC).

ATR-FTIR spectra of uncured and printed materials $S_{80}M_{20}$ with post-treatment

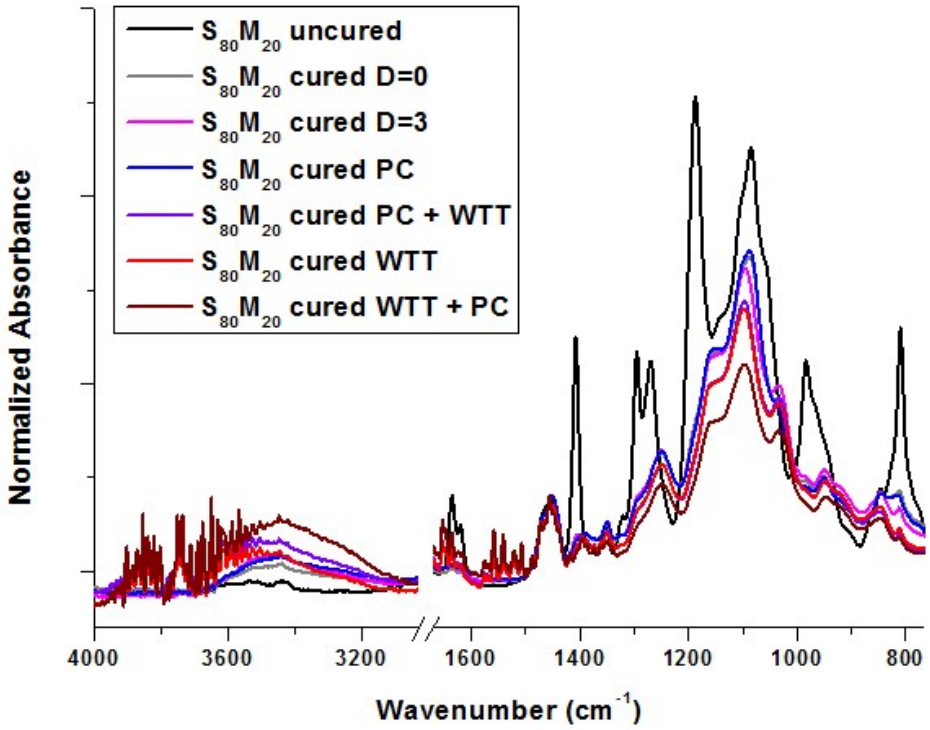

Fig. S11. ATR-FTIR spectra of the uncured formulation and the center of the $S_{80}M_{20}$ printed samples. Measurements were made directly after the 3D printing (D=0), 3 days after (D=3) or after post-treatments (PC, WTT or TT). Spectra were normalized to the reference band at 1460 cm^{-1}.

Table S5. Area obtained after integration of the ATR-FTIR band at 3600-3100 cm^{-1} and the shoulder at 1030 cm^{-1} for the uncured $S_{80}M_{20}$ and on the inner part of the printed material without PT (D=0, D=3) and with a post-treatment (PC, PC+WTT, WTT, WTT+PC).

3D printed $S_{80}M_{20}$ sample	Area of the vibration band	
	O-H stretching 3600 and 3100 cm^{-1}	Si-O-Si deformation Shoulder at 1030 cm^{-1}
Without PT, D=0	1.52 ± 0.22	0.03 ± 0.01
Without PT, D=3	2.95 ± 0.79	0.08 ± 0.05
PC	2.68 ± 0.79	0.03 ± 0.15
PC + WTT	10.99 ± 1.41	0.13 ± 0.02
WTT	10.93 ± 1.61	0.10 ± 0.01
WTT + PC	13.2 ± 2.62	0.15 ± 0.02

^{29}Si-NMR of the 3D printed material $S_{80}M_{20}$

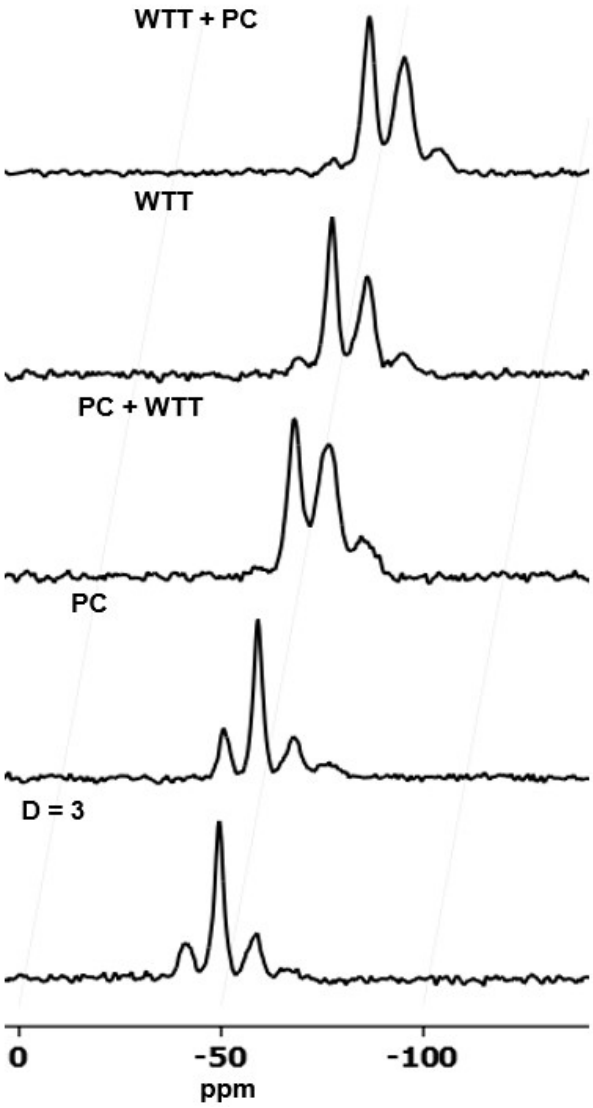

Fig. S12. ^{29}Si-NMR spectra for the material $S_{80}M_{20}$ 3 days after the 3D printing (D=3) and after post-treatments (PC, PC + WTT, WTT, WTT + PC).

Table S6. Chemical shifts attributed to the different oxo-silica substructures T^0, T^1, T^2 and T^3 from the. ^{29}Si-NMR spectra for the material $S_{80}M_{20}$ 3 days after the 3D printing (D=3) and after post-treatments (PC, PC + WTT, WTT, WTT + PC).

3D printed $S_{80}M_{20}$ samples	Chemical shift (ppm)			
	δ (T^0)	δ (T^1)	δ (T^2)	δ (T^3)
D=3	-41.6	-49.6	-58.9	-66.9
PC	-41.3	-49.8	-58.4	-67.6

PC+ WTT	-40.6	-49.6	-58.1	-68.2
WTT	-41.6	-49.6	-58.3	-67.1
WTT + PC	-40.7	-49.5	-58.2	-66.8

Storage and Young moduli obtained from DMA and tensile test at break for the printed materials $S_{80}M_{20}$ and S_{100} with or without post-treatment

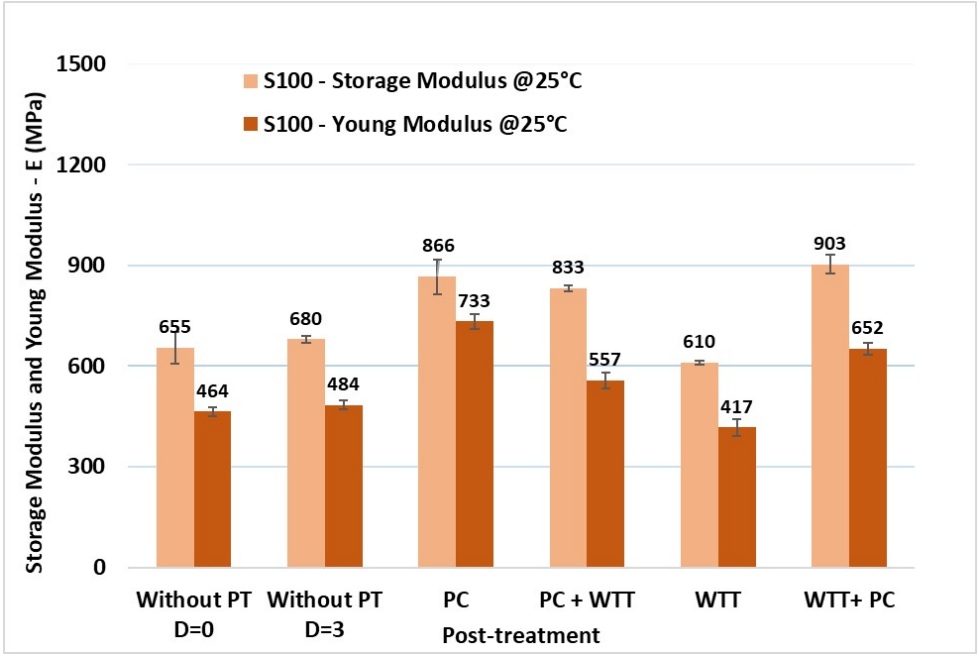

Fig. S13. Storage and Young moduli measured on the material S_{100} with DMA and tensile test at break, without post-treatment (D=0, D=3) and with implementation of post-treatment directly after 3D printing (PC, PC + WTT, WTT, WTT + PC).

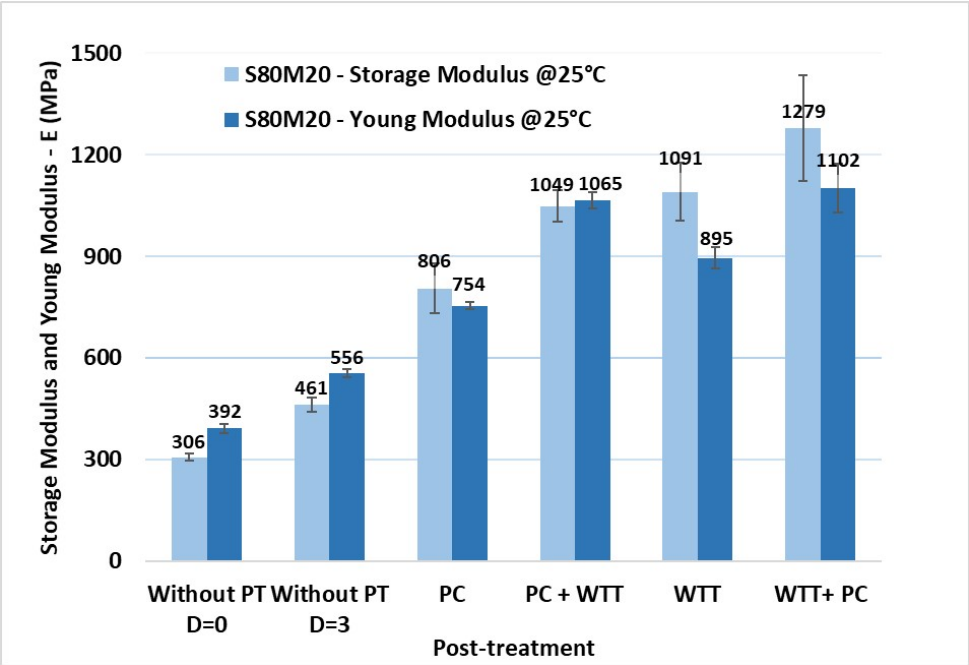

Fig. S14. Storage moduli and Young moduli measured on the material $S_{80}M_{20}$ with DMA and tensile test at break, without post-treatment (D=0, D=3) and with implementation of post-treatment directly after 3D printing (PC, PC + WTT, WTT, WTT + PC).

Tensile tests at break of S_{100} and $S_{80}M_{20}$

Table S7. Parameters (strain and stress at break) obtained by the tensile tests at break on S_{100} (4mm thick sample) directly after the 3D printing (D=0), 3 days after the 3D printing (D=3) and after post-treatments (PC, PC + WTT, WTT, WTT + PC).

3D printed S_{100} samples	ε (%)	σ (MPa)
Without PT, D=0	5.5 ± 0.7	12.7 ± 1.2
Without PT, D=3	6.3 ± 2.3	12.9 ± 1.4
PC	4.4 ± 0.5	16.4 ± 0.9
PC + WTT	5.1 ± 1.2	13.9 ± 1.4
WTT	3.8 ± 0.4	9.5 ± 1.0
WTT + PC	4.4 ± 1.3	14.5 ± 1.9

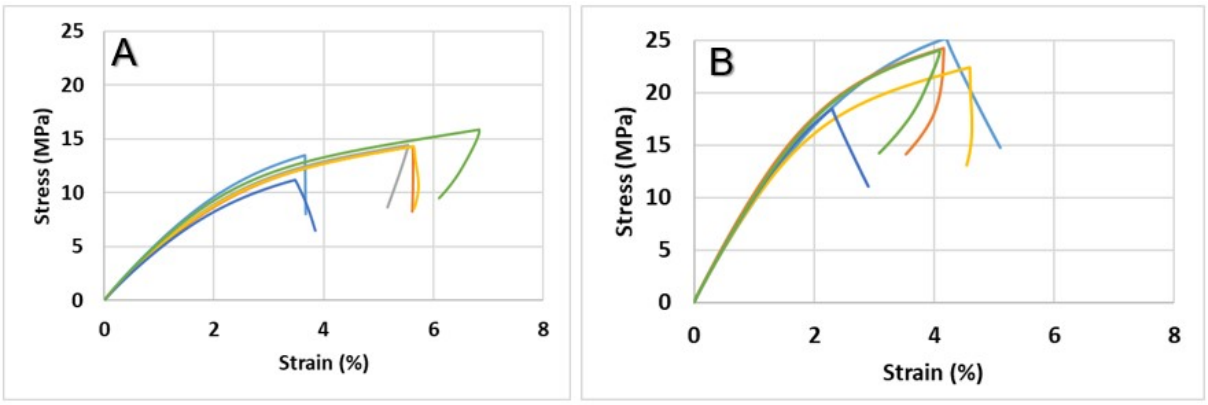

Fig. S15. Stress/Strain curve obtained by tensile test at break after PC + WTT for A) 3D printed sample S_{100} and B) $S_{80}M_{20}$. Sample thickness was of 4 mm.

Notes and references

1 J. P. Jacobs, *Rapid Prototyping & Manufacturing: Fundamentals of StereoLithography*, Society of Manufacturing Engineers, Michigan, 1992.

2 J. P. Jacobs, *Stereolithography and other RP&M Technologies: from Rapid Prototyping to Rapid Tooling*, American Society of Manufacturing Engineers, Michigan, 1995.

3 A. Champion, B. Metral, A.-S. Schuller, C. Croutxé-Barghorn, C. Ley, L. Halbardier and X. Allonas, *ChemPhotoChem*, 2021, **5**, 839–846.

4 F. de Buyl and A. Kretschmer, *J. Adhes.*, 2008, **84**, 125–142.

5 A. Bahadoor, A. Brinkmann and J. E. Melanson, *Anal. Chem.*, 2021, **93**, 851–858.